

Contents list available at CBIORE journal website

### Remarkable Energy Development

Journal homepage: https://ijred.cbiore.id



Research Article

# Renewable energy from irrigation infrastructure: Experimental insights from a Michell-Banki micro-hydropower prototype in a Colombian irrigation district

Juan Gonzalo Ardila Marín 🖲, Jean Carlos Acosta Vargas\* 🗅 , Daniela Andrea Narváez Cortes 🗅

Programa de ingeniería agrícola, Facultad de ingeniería, Universidad Surcolombiana, Neiva, Huila, Colombia

**Abstract**. This study presents the experimental characterization of a Michell–Banki micro-hydropower prototype implemented in the Tunel del Río Neiva irrigation district (Colombia), aimed at promoting distributed generation in off-grid rural areas. The system was designed for a nominal flow of 0.24 m³/s and a net head of 18 meters, capable of delivering up to 20 kW of electrical power. The turbine-generator performance was evaluated under progressive load and variable flow conditions using direct measurements of voltage, current, power, and rotor speed. A custom-built experimental resistor bank (ERB) was implemented to simulate real load scenarios, enabling the analysis of electrical response as the number of luminaires increased. The results revealed a strong linear correlation between rotor speed and generated voltage (R² = 0.9953), validating the electromechanical design. However, a saturation trend in power output was observed beyond the tenth luminaire, attributed to reduced rotor speed under load. Polynomial regression models were developed to describe the influence of flow rate on speed, voltage, and power. The cubic models for voltage and power achieved coefficients of determination above 97%, with RMSE values of 5.41 V and 375.47 W, respectively. Residual plots confirmed the validity of the models and highlighted the importance of operating close to the nominal flow rate to ensure optimal performance. This work demonstrates the feasibility of using Michell–Banki turbines for rural electrification through irrigation infrastructure. The methodology and findings provide valuable insights for future implementations, emphasizing the need for hydraulic regulation to maintain system efficiency under variable load conditions.

Keywords: Distributed generation, Energy saturation, Experimental correlation, Polynomial modeling.



@ The author(s). Published by CBIORE. This is an open access article under the CC BY-SA license (http://creativecommons.org/licenses/by-sa/4.0/).

Received: 11th August 2025; Revised: 28th Sept 2025; Accepted: 7th Oct 2025; Available online: 25th Oct 2025

#### 1. Introduction

In off-grid rural areas, limited access to conventional energy sources represents a significant obstacle to social, educational and productive development (Erdiwansyah et al., 2021). This situation especially affects agricultural communities (Bazzana et al., 2020; Chel & Kaushik, 2011; Kaygusuz, 2011). In this context, harnessing the hydraulic potential of irrigation canals through Michell-Banki type micro-hydropower plants is a viable, low-cost alternative that can be adapted to local conditions (Halder et al., 2020; Ibañez et al., 2020). These turbines, due to their robust design and capacity to operate efficiently under variable flow rates, allow the transformation of existing infrastructure into sources of distributed electricity generation (Assefa & Tesfay, 2025; Perez-Rodriguez et al., 2021). The implementation of this type of technology not only improves the quality of life of irrigation system users, but also strengthens energy self-management processes (López-González et al., 2017), promotes technological innovation in rural areas (Ibañez et al., 2020; Reyna et al., 2016) and contributes to meeting global targets such as Sustainable Development Goal (SDG) 7, which aims to ensure affordable and sustainable energy for all (Obaideen et al., 2022; Wendimu et al., 2023).

The development of Michell-Banki type micro hydropower plants has been the subject of multiple studies combining numerical, experimental, and applied design approaches. In the Colombian context, Ramírez Ramírez & Cerquera Valderrama (2020) identified a hydropower potential of more than 100 kW in the Túnel del Río Neiva irrigation district, which led to the design and evaluation of a 20 kW Michell-Banki turbine. Sotto Capera et al. (2023) complemented this work and generated characteristic curves of the prototype using CFD simulations. At the international level, Derakhshan & Nourbakhsh (2008) proposed methods to characterize pumps operating as turbines, establishing relationships between speed and efficiency that are reflected in the correlation analyses performed in this paper. Sammartano et al. (2016) and Elbatran et al. (2018) developed hydraulic and electronic regulation schemes for Banki turbines, relating parameters such as power coefficient (Cp) and tip speed ratio (TSR), which are related to the power and speed curves presented in this work. Verde et al. (2018), although focused on wind turbines, provided methodologies for estimating electromechanical losses in systems with synchronous generators, like the one used in this prototype, which helps interpret the deviations between theoretical and measured power. Tarimer & Yuzer (2011) and Vasić et al. (2018) addressed

\* Corresponding author

the design of permanent magnet generators and the selection of turbines based on operating parameters. Finally, Reyna et al. (2019) and Niyonzima & Hendrick (2021) highlighted the applicability of Michell-Banki turbines in rural and educational contexts, validating their use in experimental setups similar to the one developed in this project. This background consolidates the technical and scientific framework that supports the experimental characterization presented, and allows the results obtained to be contextualized in terms of the specialized literature.

Although Michell-Banki turbines have been widely studied for rural electrification (Mrope et al., 2021; Rahman et al., 2025; Tesfay et al., 2025), most existing research focuses on numerical simulations (Ardila Cerquera et al., 2025; Mendonça et al., 2025; Mereke et al., 2024) and laboratory-scale prototypes under idealized conditions (Macias Rodas et al., 2022; Romero-Menco et al., 2024; Sierra-Moreno et al., 2024). There is a lack of experimental studies that assess the real-world performance of these systems when integrated into existing irrigation infrastructure, particularly under progressive load and variable flow scenarios. This gap limits the development of predictive models and practical design guidelines for field implementation. This study provides an experimental characterization of a fullscale Michell-Banki micro-hydropower system installed in the Túnel del Río Neiva irrigation district, Colombia. This study is novel in its integration of hydraulic and electrical measurements under realistic operating conditions, using polynomial modeling to establish functional relationships between flow rate, rotor speed, voltage, and power. These insights contribute to the optimization of rural microgeneration systems and provide a replicable methodology for similar contexts. Specifically, the study analyzes the influence of turbine speed on the quality of the generated electrical energy, the effect of load increase on the hydraulic-mechanical system, and the correlation between valve opening and no-load speed. Characteristic curves are proposed to understand the interaction between flow, power, and voltage, validating the system design and guiding future implementations in non-interconnected rural areas.

#### 2. Method

#### 2.1. Turbine Selection Rationale

The experimental system was installed in the Túnel del Río Neiva irrigation district, in the site known as "La Parrilla", located between the municipalities of Campoalegre and Hobo (Huila, Colombia), at an altitude of approximately 611 meters

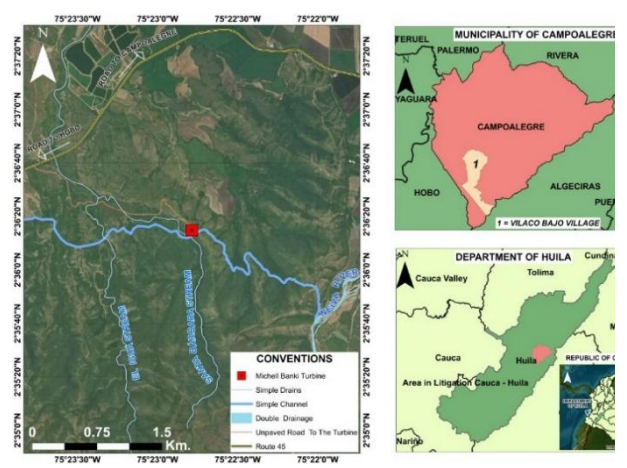


**Fig 1.** Location of the micro-hydroelectric power plant. **Source**: Sotto et al., 2026.

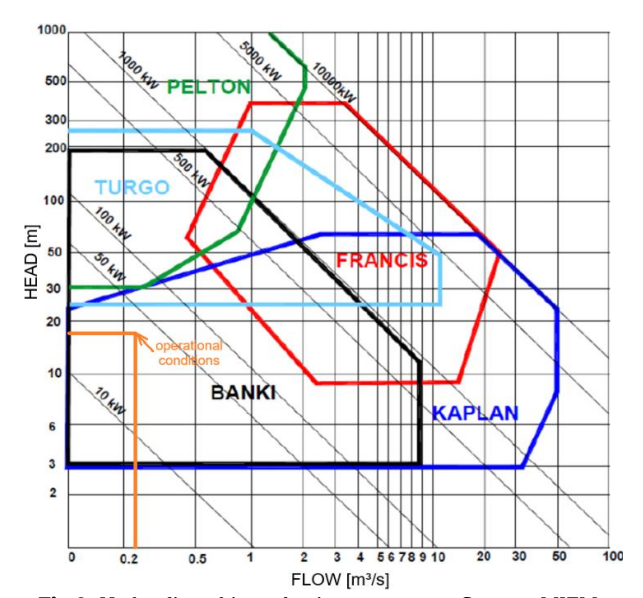


**Fig 2.** Hydraulic turbine selection nomogram. **Source**: MIEM, 2010.

above sea level, at coordinates  $2^{\circ}36'13.24$ " N and  $75^{\circ}22'46.53$ " W, based on the WGS 84 international geodetic system, as shown in Figure 1.

The selection of the Michell-Banki turbine for this project was based on a combination of hydraulic suitability, economic feasibility, and operational simplicity, particularly in the context of rural electrification under budget constraints. According to the energy potential assessment conducted by Ramírez and Cerquera (2020), the site known as "La Parrilla" in the USOIGUA irrigation district offers a flow rate ranging from 0.87 to 1.24 m<sup>3</sup>/s and a net head of 18 meters. However, the project had a demonstrative purpose, and therefore the microhydropower plant was designed to use only 0.24 m<sup>3</sup>/s of the canal flow. These conditions fall within the operational range of both Kaplan and Michell-Banki turbines, as indicated by standard nomograms used in small hydropower design (Paish, 2002; Singhal and Kumar, 2006), as shown in Figure 2, which presents the standard turbine selection nomogram (head vs. flow), highlighting the project's operating point and the Michell-Banki domain. While Kaplan turbines generally offer higher hydraulic efficiency, their design, manufacturing, and maintenance requirements are more complex and costly. In contrast, the Michell-Banki turbine presents a more accessible alternative due to its simpler construction, low maintenance requirements, and adaptability to variable flow conditions. These characteristics make it particularly suitable for rural applications where technical resources and financial capacity are limited (Drinkwaard et al., 2010). The decision to implement a Michell-Banki turbine was further supported by the project's funding limitations and the need for a replicable model that could be adopted in similar rural contexts.

#### 2.2. Microhydro system design and implementation

The site offers a net head of 18 meters, and the prototype was designed for a flow rate of 0.24 m³/s to generate approximately 20 kW of electric power. The system includes a lateral intake, a 12-inch-diameter PVC penstock, and a synchronous generator, all integrated into a reinforced structural frame designed to withstand static and dynamic loads (Sotto *et al.*, 2026). The hydraulic and structural components

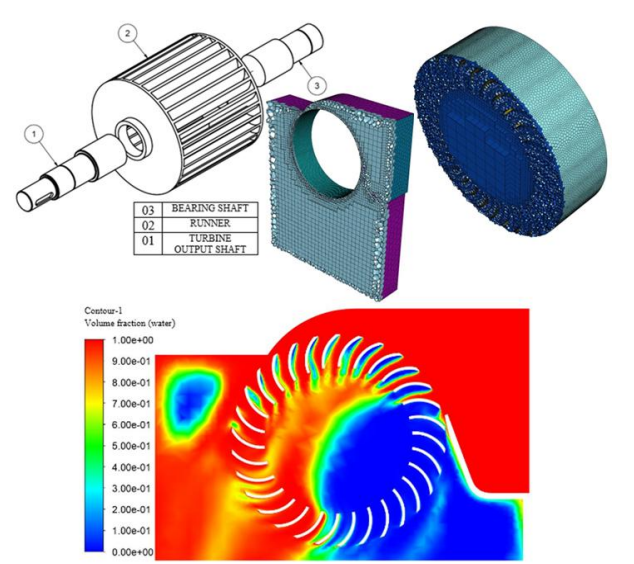


**Figure 3.** CAD of the turbine rotor, simulated control volume meshes, and CFD results of the performance study. **Source**: Sotto, *et al.*, 2023.

were developed following both empirical guidelines and national construction codes (NSR-10). The civil infrastructure includes a intake box, a buried pipeline with concrete anchors spaced every 12 meters, and a turbine housing mounted above the irrigation canal. The structural design was validated using SAP2000 software, ensuring compliance with seismic, wind, and thermal load combinations.

The hydraulic and mechanical design of the turbine was carried out following OLADE (1988) recommendations. To optimize turbine performance, a detailed numerical study was conducted using Computational Fluid Dynamics (CFD). The study evaluated the influence of the injector's opening angle on turbine efficiency, using a k-ω turbulence model and polyhedral mesh to ensure simulation accuracy (Sotto et al., 2023). The CFD simulations highlighted the importance of blade orientation and injector geometry. The turbine was designed with 30 blades and a diameter ratio of 0.66. However, the use of second-hand oil pipes for blade construction introduced deviations from ideal curvature, which may explain the discrepancy between theoretical and actual performance. Despite this, the design was deemed feasible, and the turbine was built and tested under real conditions as described in the following sections, validating the numerical predictions and confirming the system's suitability for rural applications. Figure 3 illustrates the rotor geometry, the control volume meshing



**Figure 4.** Presentation of turbine components: Rotor – Casing – Structure, in the metalworking manufacturing workshop.



**Figure 5.** Fluid inlet box, hydraulic transmission line, and details of the turbine transition and installation.

strategy employed for the numerical analysis, and representative results from the performance study. These visualizations, adapted from Sotto *et al.* (2023), offer valuable insights into the interaction between the working fluid and the turbine blades, supporting the design choices and performance evaluation.

After completing the design phase, the construction and installation of the Michell-Banki micro-hydropower system were carried out, adapting the project to the site's specific hydraulic and topographic conditions. The Michell-Banki turbine and its casing were fabricated using structural steel, with critical components such as the rotor and blades manufactured from A36 steel and assembled according to detailed CAD drawings. The fabrication process involved CNC plasma cutting, precision welding, and dynamic balancing of the rotor to minimize vibrations during operation (Figure 4).

The intake structure was built using reinforced concrete to ensure reliable water capture, and a 12-inch PVC pipeline was installed underground to convey water from the intake to the turbine. Special attention was given to the anchoring of the pipeline, with concrete blocks placed at regular intervals to prevent displacement due to hydraulic forces and terrain slope (see Figure 5). The transition between the pipeline and the turbine injector required on-site adjustments to account for dimensional variations, ensuring a watertight and efficient connection. The assembled turbine was mounted on a steel support structure designed to withstand both static and dynamic loads. The alignment of the turbine, transmission system, and generator was carefully verified to optimize power transfer and minimize mechanical losses (Figure 5). Commissioning of the system included the installation of a custom-built test bench equipped with resistive loads and realtime monitoring sensors to evaluate the electrical output under various load conditions, as described in the following section.

#### 2.3. General description of the experimental procedure

The system includes a lateral intake above the sand trap, a 12-inch-diameter, 60-meter-long PVC pipeline, a manually operated 9-position butterfly valve, a V-belt drive system and a three-phase synchronous generator of the STC type. To characterize the electrical performance of the turbine-generator



Figure 6. Experimental resistance bench (ERB) plate.

set, an experimental resistor bank (ERB) was designed and implemented to simulate progressive load conditions through the sequential activation of halogen lamps.

The ERB was designed as a tool to evaluate the generator under controlled load conditions, following criteria established in standards such as IEEE Std 115-2019 e ISO 8528-1. The bank consists of 20 halogen lamps distributed in four columns: the first two columns contain 12 bulbs of 1500 W each (18,000 W total), and the remaining two contain 8 bulbs of 500 W each (4,000 W), reaching a maximum load of 22,000 W, equivalent to 110 % of the generator's rated power. The lamps are activated using dust-protected rocker switches. All components are mounted on a  $1.1 \times 0.5$  m slanted metal plate, mounted on a modular steel frame with elevated rear legs for improved visibility and operation. The system includes a three-phase 40 A thermomagnetic circuit breaker and AWG 10 type THHN wiring, sized according to NTC 2050. Figure 6 shows the plate where the bench elements are embedded.

To measure the rotational speed of the turbine rotor and the driving and driven pulleys, a digital photographic tachometer (TFD) was used, applying reflective tape at the measurement points. The phase-to-phase and line voltages of the generator were measured with a Uni-T UT890D multimeter. For the calculation of the electrical power, a FLUKE 323 True RMS multimeter was used, recording current and voltage at the ERB's input terminals.

The tests were performed under two main conditions: no load (luminaires off) and progressive load (sequential lighting of luminaires). On each experimental day, the butterfly valve was adjusted from positions 1 to 8, making it possible to evaluate the effect of the flow rate on the turbine speed and electrical generation. In the tests with load, the valve opening was kept fixed (position 5 or 6) and the lamps were activated sequentially, recording voltage, current and speed at each step. In no-load tests, the rotor speed was measured as a function of valve opening to establish the hydraulic response curve of the system. A stabilization time of 60 seconds was allowed after each setting before taking the measurements.

#### 2.4. Data processing and analysis

The analysis of the data obtained in the field was performed using a spreadsheet to perform statistical regression. The objective was to characterize the behavior of the turbine-generator system under progressive load conditions, correlating variables such as the number of activated lamps, rotor speed, line voltage, and generated electrical power.

Unlike conventional three-phase systems, the ERB operates with two-phase lamps connected between two generator phases. Therefore, the electrical power was not calculated using the conventional three-phase formula but rather using Equation (1).

$$P = V_f I \tag{1}$$

where:  $V_f$  is the phase-to-phase voltage supplying each lamp as it was progressively activated, measured either at the generator terminals or at the input of the totalizer, as previously described. I is the input current to the ERB on either of the two lines supplying the activated lamp. Each luminaire has a power rating (1500 W or 500 W), but the actual voltage measured in the field varied as they were turned on, which affects actual power consumption, as discussed later. To obtain the total accumulated power, the individual power consumptions of each activated lamp were summed, considering the actual voltage at each step. The results were used to construct a 3D graph relating to the number of luminaires lit, the electrical power consumed by each luminaire and the total electrical power consumed, which was considered equivalent to the generated power.

To estimate the percentage of flow entering the turbine in each butterfly valve opening position, the flow coefficient  $K_{\nu}$  corresponding to valves of 300 mm nominal diameter was used, according to the manufacturer's technical specifications. The value of  $K_{\nu}$  represents the water flow (in  $m^3/h$ ) through the valve at a pressure drop of 1 bar. The values of  $K_{\nu}$  were taken for each degree of opening (from  $0^{\circ}$  to  $90^{\circ}$ ) and normalized with respect to the maximum value ( $K_{\nu}$  at  $90^{\circ}$ ), thus obtaining the relative flow rate percentage for each position. This ratio was used as a dimensionless variable in the correlation analyses between flow rate, rotor speed and electrical power generated. The procedure allowed linking the hydraulic behavior of the system with the power curves obtained experimentally, without the need to directly measure the flow rate in the field, which is especially useful in rural systems without flow instrumentation installed.

The data were organized in matrices that include the number of luminaires on (1 to 20), the turbine rotor speed (rpm), the phase-to-phase voltage, the input current to the BRE, and the total cumulative electrical power calculated as described above. In addition, the valve positions at which the required nominal voltage ( $\leq$  220 V) were achieved, and the most representative sections were selected for modeling.

As for statistical modeling, polynomial regressions of degree 1, 2 and 3 were applied to model the relationship between the electrical power generated and three independent variables, namely, the number of luminaires lit, the rotor speed, and the voltage between phases. Each regression was performed using the least squares method, using libraries such as PolynomialFeatures to generate model terms and LinearRegression to fit the coefficients. For the interpretation of the models, each model was considered to have the general form of Equation (2).

$$y = a_0 + a_1 x + a_2 x^2 + a_3 x^3 (2)$$

where: y is the dependent variable whose correlation was evaluated. x is the independent variable (e.g., regime, flow percentage)  $a_0$  is the intercept term, included only in some regressions  $a_1$ ,  $a_2$ ,  $a_3$  are coefficients indicating the sensitivity of power to changes in x.

The physical meaning of the coefficients, initially that of the linear coefficient  $a_1$  represents the change in power per unit increase in the variable, e.g., how many watts are gained per activated lamp. The quadratic coefficient  $a_2$  indicates whether the growth is accelerated or decelerated, a negative value may indicate system saturation. And the cubic coefficient  $a_3$  captures more complex effects such as fluctuations or inflection

points in the system. The coefficient of determination  $R^2$  indicates what percentage of the variability in the data is explained by the model. If  $R^2 \approx 1.0$ , the fit is considered excellent; if  $R^2 > 0.9$ , very good; and if  $R^2 < 0.7$ , weak, possibly due to noise or a non-polynomial relationship. In this study, most of the models showed values of  $R^2 > 0.94$ , which indicates a very high correspondence between the experimental parameters evaluated.

In addition to the coefficient of determination  $(R^2)$ , which is already discussed as a measure of model fit, additional statistical analyses were performed to reinforce the validity of the correlation models. For each regression (linear, quadratic, or cubic), the root mean square error (RMSE) and the residuals' standard deviation were calculated to quantify the average and typical deviations of the experimental data from the model predictions. Residual plots were generated to visually assess the distribution and randomness of the errors, to help identify potential systematic deviations or model limitations. For the linear model, a confidence interval for the slope was computed to assess the statistical significance and robustness of the relationship. These statistical tools provide a more comprehensive assessment of model performance, allowing for a transparent discussion of the variability, uncertainty, and reliability of correlations, especially considering the limited number of available experimental data points.

#### 3. Result and Discussion

## 3.1. Progressive accumulation of electrical power according to the number of luminaires

Figure 7 shows the behavior of the electrical power generated by the Michell-Banki micro power plant as a function of the number of luminaires turned on in the experimental resistor bank. Each bar represents the power consumed by a specific lamp, which decreased as additional lamps were activated, while the cumulative behavior of total power output under increasing load is better illustrated in Figure 8. This analysis showed that, although the system responds almost linearly in the first sections, after a certain point a saturation trend is observed, where the increase in power per additional luminaire begins to decrease. Sinagra *et al.* (2014) reported that the Michell-Banki turbines maintain good efficiency under varying load conditions, but the observed phenomenon is attributed to the reduction of the generator speed under increasing load, which affected the output voltage and,

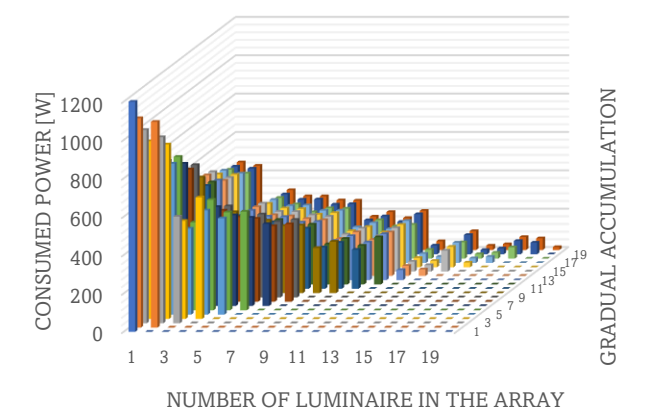


**Fig 7.** Individual and cumulative distribution of the electrical power consumed by two-phase luminaires.

consequently, the effective power delivered (discussed in the next section). The cumulative curve is key to identifying the point of maximum operating efficiency of the system, and to validate the test bed design as an energy characterization tool. These results form the basis for the regression models presented in later sections.

Figure 8 shows the combined evolution of total electrical power output and line current as the number of luminaires turned on in the experimental resistor bank increases. The blue bars represent the cumulative power calculated for each load step, while the orange bars indicate the current measured at the system input. Initially, both variables show proportional growth, reflecting an efficient response of the generating system to increased demand. However, from the tenth luminaire on, a saturation trend is observed in the power, which begins to stabilize and even decrease slightly, while the current continues to increase more steadily. Popescu & Duinea (2013) also presented efficiency and saturation curves for low-scale systems operating outside the design point. This behavior suggests that the system reaches its limiting operating regime, where the voltage begins to drop due to rotor braking, affecting the effective power delivered, which is discussed in the next section. The divergence between the two curves from this point onwards indicates that, although the system continues to demand current, the energy conversion efficiency is compromised. These results are fundamental to understanding the energy conversion phenomenon and to validate the turbinegenerator energy efficiency models.

The results presented in Figures 7 and 8 show that, under progressive load conditions, the electrical power supplied by the Michell-Banki micro-station reached a maximum of approximately 4.0 kW when the first 10 to 12 lamps were activated, stabilizing or even decreasing slightly in the final sections. This value represents just 20% of the nominal design power (20 kW), which is consistent with the hydraulic conditions under which the measurements were performed. According to Sotto et al. (2023), the system was designed to operate at 400 rpm with a flow rate of 240 L/s, however, for safety reasons, the tests were conducted with the butterfly valve set to position 5, corresponding to 28% of the maximum available flow rate. Niyonzima & Hendrick (2021) also evaluated the performance of a Michell-Banki turbine under real field conditions, including reduced flow rates. Lamesgin & Ali (2024) also discussed the impact of reduced flow on micro-hydropower plant efficiency. This hydraulic limitation resulted in an average speed of 270 rpm, which was insufficient to reach the rated voltage of 220 V under full load conditions. As a result, the power consumed per luminaire was lower than expected, and the system exhibited signs of energy saturation after the tenth

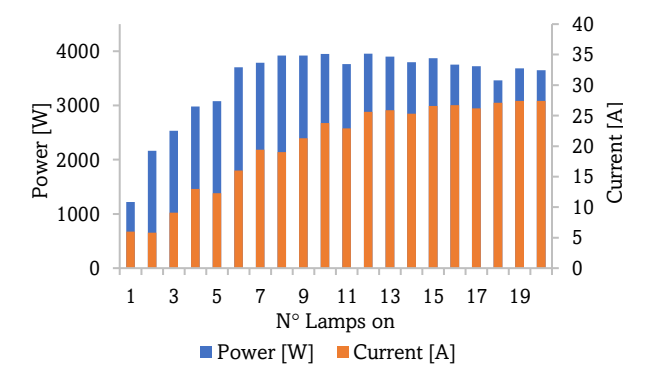


**Fig 8**. Ratio between total power supplied and line current as a function of the number of luminaires lit.

luminaire was turned on. The line current, on the other hand, continued to increase to values close to 28 A, indicating that the system was still demanding energy, but without being able to convert it efficiently into useful power. These results demonstrate the need to operate the system at hydraulic conditions close to design to achieve maximum performance and justify the implementation of flow regulation strategies for future tests.

The performance of the Michell–Banki turbine under progressive load conditions revealed a saturation trend in electrical power output beyond the tenth luminaire, attributed to reduced flow and suboptimal rotational speed. While direct efficiency measurements were not conducted, the observed behavior aligns with findings by Niyonzima & Hendrick (2021), who reported turbine efficiencies between 60% and 75% at 294 rpm under full valve opening in laboratory conditions. Their study also showed significant efficiency drops below 50% when operating at partial valve openings, consistent with the reduced performance observed in the present field tests at 28% flow. Unlike their controlled setup, the current study provides insights into real-world limitations of flow regulation and generator coupling, emphasizing the need for hydraulic control systems to maintain optimal operating conditions.

The experimental results showed a saturation trend in power output under reduced flow conditions, with significant efficiency losses when operating at less than 30% of the design flow. This behavior is consistent with the findings of Sinagra et al. (2014), who demonstrated through CFD simulations that efficiency drops when the inlet area is reduced without maintaining optimal fluid velocity. Their study proposed a semicircular segment regulation system to preserve constant hydraulic head and inlet velocity, thereby stabilizing turbine performance under variable flow. While our system lacked such regulation, the observed efficiency decline reinforces the importance of hydraulic control strategies in maintaining energy conversion efficiency in micro-hydro installations.

The efficiency behavior of the Michell-Banki turbine under reduced flow conditions exhibited a saturation trend and reduced energy conversion, particularly below 30% of the design flow. This pattern is consistent with the findings of Popescu & Duinea (2013), who evaluated a centrifugal pump operating as a turbine (PAT) and reported a peak efficiency of 65%, with stable performance above 60% at higher flow rates. Although the machine types differ, both studies underscore the sensitivity of micro-hydropower systems to flow variability and the importance of operating near the design point to achieve optimal efficiency. The comparison reinforces the need for careful hydraulic matching and flow regulation in rural energy applications. This behavior is consistent with the findings of Lamesgin & Ali (2024), who demonstrated that suboptimal geometries in Archimedes screw turbines resulted in significant power losses, even at higher flow rates. Their study showed that optimization of internal parameters such as pitch and inner radius increased efficiency from 55.4% to 92.9%. While the turbine types differ, both studies emphasize the critical role of hydraulic design and flow regulation in optimizing energy conversion in micro-hydropower systems. The comparison reinforces the need for tailored optimization strategies to adapt turbine performance to real operating conditions.

The saturation trend observed in electrical power output beyond the tenth luminaire aligns with findings by Guo et al. (2018), who demonstrated that variable-speed microhydropower systems exhibit reduced efficiency when rotational speed decreases due to increased load. Their implemented adaptive MPPT control to mitigate this effect, whereas the

present study underscores the mechanical limitations of the Michell–Banki turbine under unregulated flow conditions. This comparison reinforces the need for integrated hydraulic and electrical control systems to sustain performance under variable operating regimes.

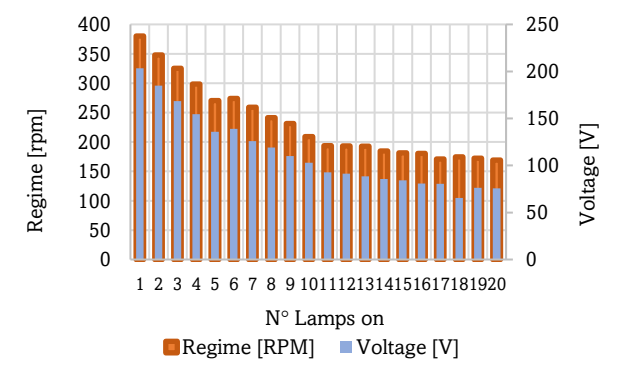
## 3.2. Influence of rotor speed on the voltage generated under progressive load.

Figure 9 presents the joint evolution of the rotational speed of the generator shaft (rpm) and the generated inter-phase voltage, as the lamps in the ERB were activated sequentially. This analysis was performed to further investigate the cause of the saturation observed in electrical power, as evidenced in the previous graphs. The orange bars represent rotor speed, while the blue bars indicate the phase-to-phase voltage supplying each activated lamp, measured at the ERB totalizer input. It is observed that, as the load increases, the speed decreases progressively. This decrease in speed results in a drop in the voltage generated, especially from the tenth luminaire on. Guo et al. (2018) discussed how variable speed affects both efficiency and generated voltage. The joint behavior of these two variables confirms that electrical power is not limited by generator capacity, but by a reduction in speed that directly affects the electromagnetic induction. This finding validates the need to implement hydraulic regulation systems that maintain the speed within optimal ranges, even under high load conditions.

Derived from the behavior shown in Figure 9, Figure 10 presents the initial correlation analysis between turbine shaft speed and phase-to-phase voltage generated by the Michell-Banki micro power plant. The data show a highly significant direct linear relationship, with Equation (3) as the fitted linear function.

$$V = 0.4953rpm \tag{3}$$

And a coefficient of determination  $R^2 = 0.9953$ , indicating that 99.53% of the voltage variability is explained by rotor speed. This result confirms that, in this system, the voltage generated depends almost exclusively on the rotational speed of the rotor, which is consistent with Faraday's law of electromagnetic induction; Sammartano et al. (2013), Sritram & Suntivarakorn (2021) and Niyonzima & Hendrick (2021) had confirmed that the generated voltage is directly related to rotor speed, especially under varying load conditions, and showed similar correlations in low-power systems for rural electrification. The positive slope of the model (0.4953) suggests that, given the direct proportionality, for every 100-rpm increase, the voltage increases approximately 49.5V, allowing



**Fig 9.** Relationship between rotor speed and voltage generated as a function of the number of luminaires lit.

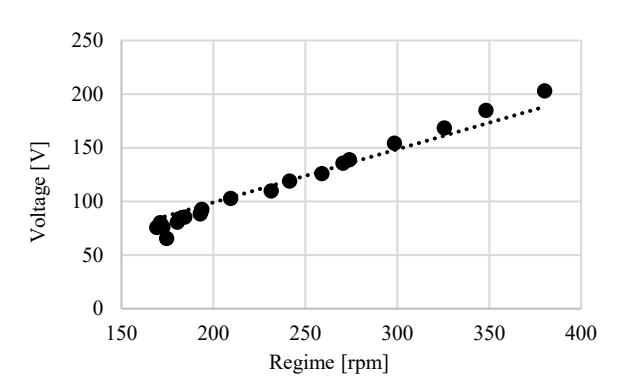


**Fig 10.** Correlation analysis between rotor speed and voltage generated in the Michell-Banki micro power plant.

estimation of system behavior under varying hydraulic conditions. This finding is key to understanding why, in the tests performed with reduced flow (valve position 5), the voltage did not reach the nominal value of 220V, limiting the effective power delivered. It further supports the need to maintain rotor speed within optimal ranges to ensure efficient power generation.

The quality of the linear fit was further assessed by calculating the root mean square error (RMSE) and the residuals' standard deviation. The RMSE, which quantifies the average magnitude of the prediction error, was found to be 8.20 V. This value indicates that, on average, the predicted voltages deviate from the measured values by approximately 8 V, which is considered acceptable given the experimental conditions and inherent system variability. The standard deviation of the residuals was 8.17 V, reflecting the typical dispersion of the errors around their mean. The similarity between the RMSE and the residual standard deviation suggests that the errors are randomly distributed and that the model does not exhibit significant bias.

To further evaluate the adequacy of the linear model, a residual plot was generated (Figure 11). The residuals, defined as the difference between the measured and predicted voltages, are plotted against rotor speed. The distribution of the residuals appears reasonably symmetric around zero, with no clear trend or curvature, indicating that the linear model is appropriate for the observed data. Although a few points exhibit larger deviations, particularly at lower speeds, the overall pattern supports the assumption of linearity and confirms the absence of systematic bias in the model.

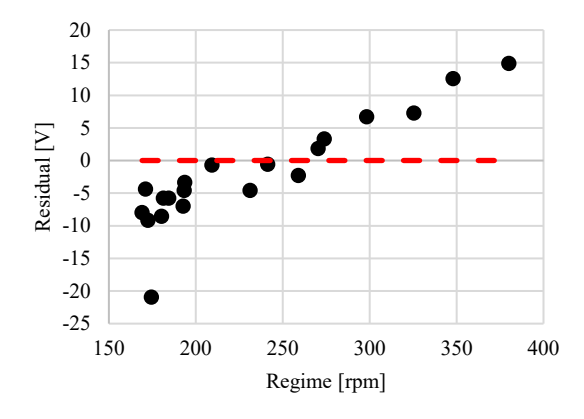


Fig 11. Residual plot: Linear model (Voltage vs. rpm).

The slope of the linear model, constrained to pass through the origin, was estimated using least squares regression and found to be 0.495 V/rpm. To assess the precision of this estimate, the slope's standard error was calculated as 0.0078 V/rpm, based on residual variance and the distribution of rotor speed as the independent variable. Using a two-tailed Student's t-distribution with 19 degrees of freedom and a 95% confidence level, the critical t-value was 2.093. This resulted in a 95% confidence interval for the slope: [0.479, 0.512] V/rpm, indicating that the relationship is statistically significant and that the slope is well constrained by the data. The narrow width of the interval supports the robustness of the model within the tested range.

The strong linear correlation between rotor speed and generated voltage (R<sup>2</sup> = 0.9953) reported in this study aligns with the electromechanical behavior described by Guo et al. (2018), who emphasized the critical role of rotational speed in determining output power and voltage in micro-hydro systems. Although Guo's setup included advanced electronic control, both studies confirm that maintaining optimal rotor speed is essential for efficient energy delivery, particularly in rural electrification contexts with limited regulation infrastructure.

#### 3.3. Variable flow studies

Figure 12 presents the behavior of the Michell-Banki turbine rotor speed under no-load conditions, as a function of the percentage of available flow (q), estimated from the butterfly valve flow coefficient, as reported by Derakhshan & Nourbakhsh (2008), Elbatran et al. (2018), and Sammartano et al. (2016) who reported regime versus flow rate curves fitted with polynomial or nonlinear models. The experimental data show an increasing trend of the regime as the flow rate increases, with a quadratic polynomial fit curve defined by Equation (4).

$$rpm = -714.83q^2 + 1184.7q \tag{4}$$

The coefficient of determination  $R^2=0.9472$  indicates that the model explains 94.72~% of the observed variability, which validates its use to characterize the hydraulic behavior of the system. The negative quadratic term suggests the existence of a peak efficiency point in rotor speed, beyond which the increase in flow rate does not translate into a proportional increase in velocity, possibly due to effects such as turbulence, cavitation or friction losses. This model allows the identification of the optimal range of hydraulic operation to maximize rotor speed under no-load conditions, which is key to ensure adequate electrical generation when the system is connected to the resistor bank.

The largest residuals occur at 16.8% and 10.0% flows rates, where the model overestimates rotor speed, while at 28.5% and 100% flow, the predictions are closer to the measured values. These residuals reflect the nonlinearity of the system and the influence of hydraulic and mechanical factors not captured by the model. Nevertheless, the quadratic fit provides a reasonable approximation of the system behavior under variable flow conditions and supports the use of this model for estimating performance within the tested range.

The RMSE, which quantifies the average magnitude of the prediction error, was 51.81 rpm. This means that, on average, the predicted rotor speed deviates from the measured values by approximately 52 rpm across the tested flow rates. The standard deviation of the residuals was 55.0 rpm, indicating the typical dispersion of the errors around their mean. These statistical

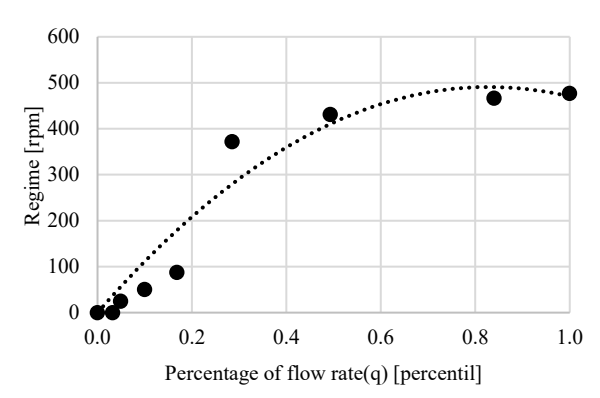
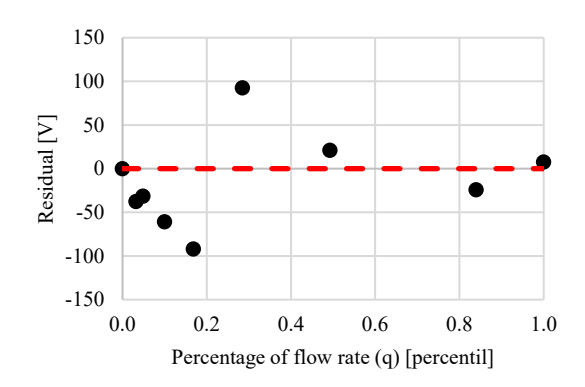


Fig 12. Unloaded rotor speed behavior as a function of available flow rate.



**Fig 13.** Residuals of the quadratic fit for rotor speed as a function of flow rate.

indicators provide a complementary perspective on the model's highlighting both the accuracy and consistency of the predictions within the experimental range.

Figure 13 shows the residuals of the quadratic fit as a function of the normalized flow rate. The distribution of the residuals does not reveal a clear systematic pattern, although some larger deviations were observed at intermediate flow rates. This suggests that, while the quadratic model captures the overall trend of the data, there are specific conditions where the experimental variability is not fully explained by the model. Nevertheless, the residuals remain within a reasonable range, supporting the adequacy of the quadratic fit for describing the relationship between flow rate and rotor speed within the tested interval.

Figure 14 shows the behavior of the inter-phase voltage generated by the Michell-Banki micro-hydropower plant as a function of the percentage of available flow, under full load conditions (20 lamps activated). Verde et al. (2018) reported voltage versus speed curves for synchronous generators with fitted cubic models. The fitted model is a third-degree polynomial function, defined by Equation (5).

$$V = 206.25q^3 - 457.53q^2 + 346.23q (5)$$

The coefficient of determination  $R^2 = 0.9798$  indicates that the model explains 97.98 % of the observed variability, which validates its use to represent the behavior of the system under real operating conditions. The positive cubic term suggests that voltage increases at an accelerated rate at higher flow levels, while the negative quadratic term indicates a transition zone

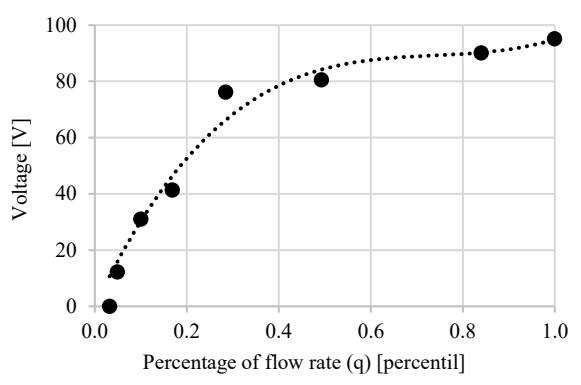


Fig 14. Voltage curve generated as a function of the percentage of flow rate at full load.

where the system efficiency declines, likely due to turbulence, cavitation, or hydraulic losses. This nonlinear behavior reflects the complexity of the interaction between the hydraulic flow and the electromechanical response of the generator, and helps identify the optimal flow rate range to achieve the rated voltage of 220 V. The model also shows that, at reduced flow conditions (at less than 50%), the voltage generated is insufficient to supply nominal loads, reinforcing the need to operate the system near its hydraulic design point.

The residuals remain within an acceptable range for most flow rates, although larger discrepancies are observed at the lowest flow settings, likely due to increased hydraulic losses or measurement uncertainty. Overall, the results support the suitability of the cubic model for representing the voltage response of the system as a function of hydraulic input.

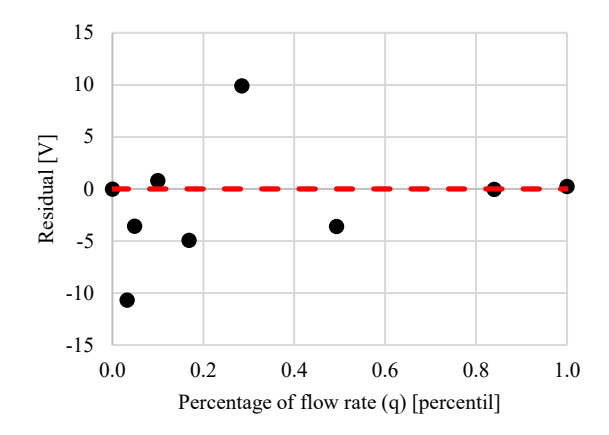
The RMSE of the residuals was 5.41 V. The standard deviation of the residuals was 5.56 V, reflecting the typical dispersion of the errors around their mean. These values confirm the reliability of the cubic model within the tested flow range and support its use for estimating voltage behavior under full load conditions.

Figure 15 shows the distribution of the residuals from the cubic voltage model as a function of the normalized flow rate. The red dashed line at zero serves as a reference for perfect model fit. The residuals are generally symmetrically distributed around zero, with no clear systematic trend or curvature, confirming that the cubic model adequately represents the relationship between flow rate and voltage within the tested range. However, slightly larger deviations are observed at the lowest and intermediate flow rates, which may be attributed to increased hydraulic losses or measurement uncertainties under these conditions.

Figure 16 shows the behavior of the electrical power generated by the Michell-Banki micro power plant as a function of the percentage of available flow, under full load conditions (20 lights on). The fitted model is a third-degree polynomial function, defined by Equation (6).

$$V = -750.89q^3 - 6769.8q^2 + 12280q (6)$$

The coefficient of determination  $R^2 = 0.9721$  indicates that the model explains 97.21% of the observed variability, which validates its use to represent the behavior of the system under real operating conditions. The positive cubic term suggests that power increases at an accelerated rate towards the upper end of the flow range, while the negative quadratic term indicates a transition zone where the system loses efficiency, possibly due to hydraulic saturation effects, turbulence or generator

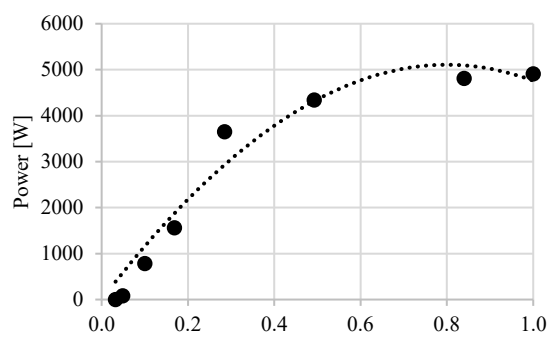


**Fig 15.** Residuals of the cubic voltage model as a function of normalized flow rate under full load conditions.

limitations. This model identifies the optimum flow range to maximize the power output, and shows that, at low flow conditions (below 30%), the power generated is less than 2 kW, well below the nominal design capacity (20 kW). These results reinforce the need to operate the system close to its hydraulic design point to ensure efficient energy conversion.

The cubic regression between flow rate and electrical power output confirms the nonlinear behavior of the turbine-generator system under full load conditions. While the present study is based on field measurements, Sammartano et al. (2013) conducted CFD simulations to optimize the geometry of Michell-Banki turbines, reporting peak efficiencies above 88% for impellers with 35 blades and an attack angle of 22°. Their results showed that efficiency remains above 80% across a wide range of flow rates, which aligns with the saturation trend observed in our experimental data. However, unlike their conditions, our system exhibited reduced performance at low flow rates due to hydraulic limitations and generator coupling losses. This comparison highlights the importance of integrating geometric optimization with realworld constraints to achieve reliable energy conversion in rural micro-hydro systems.

The RMSE was 375.47 W, indicating that the predicted power values deviate from the measured values by approximately 375 W. The standard deviation of the residuals was 381.47 W, reflecting the typical dispersion of the errors around their mean. These values confirm the reliability of the cubic model within the tested flow range and support its use for



Percentage of flow rate(q) [percentil]

**Fig 16.** Curve of electrical power generated as a function of the percentage of flow rate at full load.

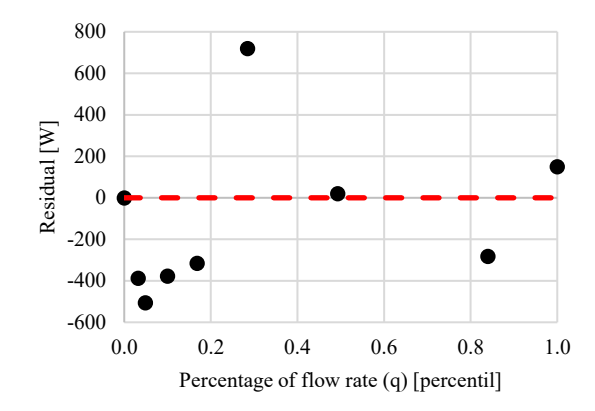


**Fig 17.** Residuals of the cubic power model as a function of normalized flow rate under full load conditions.

estimating the power output of the system under full load conditions.

Figure 17 illustrates the distribution of residuals from the cubic power model (Equation 6) as a function of the normalized flow rate. Each blue dot represents the deviation between the measured and predicted power at a given flow rate, while the red dashed line at zero serves as a reference for ideal model fit. The residuals are generally distributed around the zero line, with no evident systematic bias, indicating that the model adequately captures the nonlinear relationship between flow rate and power output. However, greater deviations are observed at low and intermediate flow rates, which may be attributed to hydraulic inefficiencies, generator response limitations, or measurement variability. Overall, the residual plot supports the robustness of the cubic model within the tested range and reinforces its suitability for estimating power generation under full load conditions.

The polynomial regression models developed in this study to correlate flow rate with rotor speed, voltage, and electrical power exhibit similar behavior to the models proposed by Guo et al. (2018), who employed regression techniques based on Hill Chart measurements to characterize the efficiency of microhydro turbines. Both approaches reveal nonlinear trends and saturation effects when operating outside the design point, underscoring the importance of hydraulic regulation to maintain optimal energy conversion. While Guo's work focused on simulation and control strategies, the present study validates these patterns through field-based experimentation under realistic load and flow conditions.

Polynomial regression models applied in this study to correlate flow rate, rotor speed, and voltage with power output align with the modeling approach used by Sritram and Suntivarakorn (2021), who employed Response Surface Methodology (RSM) to optimize turbine blade configurations. Both studies confirm that nonlinear models are effective in capturing the complex interactions between hydraulic and mechanical parameters in micro-hydro systems. They are also consistent with the approach proposed by Derakhshan and Nourbakhsh (2008), who derived second- and third-order polynomial equations to estimate the complete characteristic curves of centrifugal pumps operating as turbines. Both studies emphasize the importance of modeling off-design performance to support field implementation in small hydro sites.

Other studies have addressed the modeling of electromechanical systems using regression techniques, such as the works by Wu *et al.* (2018), Siavash *et al.* (2021), and Balacco (2018), which apply polynomial models and artificial neural

networks to estimate parameters of induction machines, wind turbines with variable ducts, and pumps operating as turbines, respectively. While they share a focus on correlating hydraulic and electrical variables, these studies are mostly based on simulated environments or normalized data, which justifies the need for research like the present one, grounded in real field measurements. However, to deepen this work, it would be advisable to incorporate artificial intelligence techniques such as neural networks or evolutionary regression, which could enhance the predictive capacity of the model and explore more complex nonlinear relationships among system variables.

#### 4. Conclusion

The experimental characterization of the Michell–Banki micro-hydropower system installed in a Colombian irrigation district was consistent with the principles of hydraulic-electric conversion. The system showed a strong linear correlation between rotor speed and generated voltage ( $R^2=0.9953$ ), validating the electromechanical design and confirming that voltage output is linearly dependent on rotor speed.

Under progressive load conditions, the electrical power output showed a saturation trend beyond the tenth luminaire, reaching a maximum of approximately 4.0 kW (only 20% of the nominal design capacity). This limitation was attributed to reduced flow conditions during testing (28% of maximum), which prevented the system from reaching its optimal operating speed.

Polynomial regression models were effectively applied to describe the influence of flow rate on rotor speed, voltage, and power. The cubic models achieved coefficients of determination above 97%, with RMSE values of 5.41 V for voltage and 375.47 W for power. Residual plots confirmed the robustness of the models and emphasized the need to operate close to the design flow rate to ensure efficient energy conversion.

The study addresses a critical gap in the literature by providing field-based experimental data on the performance of Michell–Banki turbines integrated into existing irrigation infrastructure. The methodology (based on direct measurements and progressive load testing) offers a reproducible framework for future rural electrification projects. It is recommended that hydraulic regulation systems be implemented to ensure rotor speed remains within optimal ranges, especially under variable load conditions, to maximize system efficiency and reliability.

#### Acknowledgments

The authors express their sincere gratitude to Universidad Surcolombiana for the institutional support and resources provided for the development of this research. Likewise, special recognition is given to the USOIGUA Users Association for their valuable collaboration, willingness and contribution of information, which were fundamental for the realization of this work.

**Author Contributions**: **A.M.**: Conceptualization, methodology, formal analysis, resources, project administration, writing—original draft, **A.V.**; supervision, writing—original draft, validation, writing—review and editing **N.C.**; writing—review and editing, project administration, validation. All authors have read and agreed to the published version of the manuscript.

Conflicts of Interest: The authors declare no conflict of interest.

#### References

- Ardila Cerquera, M. S., Ávila Parada, M. M., Martínez Palmeth, L. H., Ardila Marín, J. G., & Acosta Vargas, J. C. (2025). Evaluation of the influence of the number of blades on a Michell Banki turbine on the power generated under given flow and head conditions. EUREKA: Physics and Engineering, (3), 27-35. https://doi.org/10.21303/2461-4262.2025.003702
- Assefa, E. Y., & Tesfay, A. H. (2025). Effect of Blade Profile on Flow Characteristics and Efficiency of Cross-Flow Turbines. *Energies*, 18(12). https://doi.org/10.3390/en18123203
- Balacco, G. (2018). Performance prediction of a pump as turbine: Sensitivity analysis based on artificial neural networks and evolutionary polynomial regression. *Energies*, 11(12), 3497. https://doi.org/10.3390/en11123497
- Bazzana, D., Zaitchik, B., & Gilioli, G. (2020). Impact of water and energy infrastructure on local well-being: an agent-based analysis of the water-energy-food nexus. *Structural Change and Economic Dynamics*, 55, 165–176. https://doi.org/10.1016/j.strueco.2020.08.003
- Chel, A., & Kaushik, G. (2011). Renewable energy for sustainable agriculture. *Agronomy for Sustainable Development*, 31(1), 91–118. https://doi.org/10.1051/agro/2010029
- Derakhshan, S., & Nourbakhsh, A. (2008). Experimental study of characteristic curves of centrifugal pumps working as turbines in different specific speeds. *Experimental Thermal and Fluid Science*, 32(3), 800–807. https://doi.org/10.1016/j.expthermflusci.2007.10.004
- Elbatran, A. H., Yaakob, O. B., Ahmed, Y. M., & Shehata, A. S. (2018). Numerical and experimental investigations on efficient design and performance of hydrokinetic Banki cross flow turbine for rural areas. *Ocean Engineering*, 159(May), 437–456. https://doi.org/10.1016/j.oceaneng.2018.04.042
- Erdiwansyah, Mahidin, Zaki, M., Asr, G., Muhibbuddin, & Jalaluddin. (2021). A review of renewable energy mini-grid systems in the non-interconnected rural areas: A case study. *Journal of Hunan University (Natural Science)*, 48(1), 133–151. http://www.jonuns.com/index.php/journal/article/view/492
- Guo, B., Bacha, S., Alamir, M., & Mohamed, A. (2018). Variable speed micro-hydro power generation system: Review and Experimental results. SYMPOSIUM DE GENIE ELECTRIQUE (SGE 2018), 3–5. https://hal.science/hal-02981922v1
- Halder, P., Doppalapudi, A. T., Azad, A. K., & Khan, M. M. K. (2020). Efficient hydroenergy conversion technologies, challenges, and policy implication. In *Advances in Clean Energy Technologies*. Elsevier Inc. https://doi.org/10.1016/B978-0-12-821221-9.00007-4
- Ibañez, L., Escobar, L., Hidalgo, A., Gordón, C., & Cumbajín, M. (2020). Michell-Banki a Promise Turbine for Pico-Hydro in Water Irrigation Channel Lenin. Applied Technologies, First International Conference, ICAT 2019, 305–317. https://doi.org/10.1007/978-3-030-42531-9
- Kaygusuz, K. (2011). Energy services and energy poverty for sustainable rural development. *Renewable and Sustainable Energy Reviews*, 15(2), 936–947. https://doi.org/10.1016/j.rser.2010.11.003
- Lamesgin, H. B., & Ali, A. N. (2024). Optimization of screw turbine design parameters to improve the power output and efficiency of micro-hydropower generation. *Cogent Engineering*, 11(1). https://doi.org/10.1080/23311916.2024.2327906
- López-González, A., Domenech, B., Gómez-Hernández, D., & Ferrer-Martí, L. (2017). Renewable microgrid projects for autonomous small-scale electrification in Andean countries. *Renewable and Sustainable Energy Reviews*, 79(September 2016), 1255–1265. https://doi.org/10.1016/j.rser.2017.05.203
- Macias Rodas, C. A., Lopez de Paz, P., Lastres Danguillecourt, O., & Ibáñez Duharte, G. (2022). Analysis and optimization to a test bench for Micro-hydro-generation. Energy Reports, 8, 321-328. https://doi.org/10.1016/j.egyr.2022.10.292
- Mendonça, P. E., Trevisan, K., da Silva, H. T., Freitas, L. F., Santos, B. R., Camps, I., & Ferreira, T. A. A. (2025). Use of water supply for microgeneration of electricity in buildings and residential. OBSERVATÓRIO DE LA ECONOMÍA LATINOAMERICANA, 23(5), e10106. https://doi.org/10.55905/oelv23n5-184
- Mereke, N. B., Ancha, V. R., & Hendrick, P. (2024). Numerical modeling and CFD simulation of diffuser augmented dual vertical axis hydrokinetic Banki-Michell turbine. Heliyon, 10(5). https://doi.org/10.1016/j.heliyon.2024.e26970

- Mrope, H. A., Chande Jande, Y. A., & Kivevele, T. T. (2021). A review on computational fluid dynamics applications in the design and optimization of crossflow hydro turbines. Journal of Renewable Energy, 2021(1), 5570848. https://doi.org/10.1155/2021/5570848
- Niyonzima, J. B., & Hendrick, P. (2021). Lab performance testing of a small Banki-Michell hydraulic turbine for remote applications. *Journal of Renewable Energies*, 24, 244–260. https://doi.org/10.54966/jreen.v24i2.984
- Obaideen, K., Yousef, B. A. A., AlMallahi, M. N., Tan, Y. C., Mahmoud, M., Jaber, H., & Ramadan, M. (2022). An overview of smart irrigation systems using IoT. *Energy Nexus*, 7(July), 100124. https://doi.org/10.1016/j.nexus.2022.100124
- Perez-Rodriguez, A. J., Sierra-Del Rio, J., Grisales-Noreña, L. F., & Galvis, S. (2021). Optimization of the efficiency of a michell-banki turbine through the variation of its geometrical parameters using a pso algorith. WSEAS Transactions on Applied and Theoretical Mechanics, 16, 37–46. https://doi.org/10.37394/232011.2021.16.5
- Popescu, D., & Duinea, A. (2013). Study of Centrifugal Pump Operating as Turbine in Small Hydropower Plants Faculty of Electrical Engineering. In *Recent Researches in Electric Power and Energy Systems* (pp. 285–288).
- Rahman, M. F. A., Kamal, N. A., Abdullah, J., Quaranta, E., & Shin, S. (2025). Unlocking the potential of micro-hydropower in water distribution networks: a comprehensive systematic review for Malaysia's sustainable energy future. Discover Sustainability, 6(1), 56. https://doi.org/10.1007/s43621-025-00818-5
- Ramírez Ramírez, L. M., & Cerquera Valderrama, C. (2020). Estudio del potencial energético de un canal ubicado en el distrito de riego USOIGUA municipio de Campoalegre-Huila, para la generación de energía eléctrica mediante la implementación de una turbina [Universidad Surcolombiana]. http://repositoriousco.co:8080/jspui/handle/123456789/5707
- Reyna, T., Irazusta, B., Reyna, S., Labaque, M., & Riha, C. (2019).

  Development of Micro Hydro Turbines As Renewable Energy Applications for Educational Purposes. *Proceedings of the IAHR World Congress*, 5949–5959. https://doi.org/10.3850/38WC092019-1426
- Reyna, T., Reyna, S., Lábaque, M., Riha, C., & Groso, F. (2016). Applications of Small Scale Renewable Energy. *Journal of Business and Economics*, 7(2), 258–266. https://doi.org/10.15341/jbe(2155-7950)/02.07.2016/008
- Romero-Menco, F., Pineda-Aguirre, J., Velásquez, L., Rubio-Clemente, A., & Chica, E. (2024). Effects of the Nozzle Configuration with and without an Internal Guide Vane on the Efficiency in Cross-Flow Small Hydro Turbines. Processes, 12(5), 938. https://doi.org/10.3390/pr12050938
- Sammartano, V., Aricò, C., Carravetta, A., Fecarotta, O., & Tucciarelli, T. (2013). Banki-Michell optimal design by computational fluid dynamics testing and hydrodynamic analysis. *Energies*, 6(5), 2362–2385. https://doi.org/10.3390/en6052362
- Sammartano, V., Filianoti, P., Sinagra, M., Tucciarelli, T., Scelba, G., & Morreale, G. (2016). Coupled Hydraulic and Electronic Regulation for Banki Turbines. *Procedia Engineering*, 162, 419–425. https://doi.org/10.1016/j.proeng.2016.11.083

- Siavash, N. K., Ghobadian, B., Najafi, G., Rohani, A., Tavakoli, T., Mahmoodi, E., & Mamat, R. (2021). Prediction of power generation and rotor angular speed of a small wind turbine equipped to a controllable duct using artificial neural network and multiple linear regression. Environmental research, 196, 110434. https://doi.org/10.1016/j.envres.2020.110434
- Sierra-Moreno, D., Romero-Menco, F., Velásquez-García, L. I., Rubio-Clemente, A., & Chica-Arrieta, E. (2024). Recomendaciones para la realización y análisis de pruebas experimentales en turbinas hidráulicas tipo Michell-Banki. Revista UIS Ingenierías, 23(2), 47-70. https://doi.org/10.18273/revuin.v23n2-2024004
- Sinagra, M., Sammartano, V., Aricò, C., Collura, A., & Tucciarelli, T. (2014). Cross-Flow turbine design for variable operating conditions. *Procedia Engineering*, 70, 1539–1548. https://doi.org/10.1016/j.proeng.2014.02.170
- Sotto Capera, F., Ardila Marín, J. G., & Cerquera Sandoval, C. (2023). Numerical Study of the Opening Angle Incidence in Michell-Banki Turbine's Performance without Guide Blades. *International Journal of Engineering Research in Africa*, 67, 101–122. https://doi.org/10.4028/p-EO6We7
- Sotto Capera, F., Cerquera Sandoval, C., Acosta Vargas, J. C., & Ardila Marín, J. G. (2026). Fluid handling and civil structure of a minihydroelectric power plant project in an irrigation district in Colombia. *REM International Engineering Journal*, 79(1), 1–14. http://dx.doi.org/10.1590/0370-44672025790042
- Sritram, P., & Suntivarakorn, R. (2021). The efficiency comparison of hydro turbines for micro power plant from free vortex. *Energies*, 14(23). https://doi.org/10.3390/en14237961
- Tarimer, I., & Yuzer, E. O. (2011). Designing of a permanent magnet and directly driven synchronous generator for low speed turbines. *Elektronika Ir Elektrotechnika*, 6(6), 15–18. https://doi.org/10.5755/j01.eee.112.6.436
- Tesfay, A. H., Weldemariam, S. A., & Gebrelibanos, K. G. (2025). Design and Development of Crossflow Turbine for Off-Grid Electrification. Energies, 18(19), 5108. https://doi.org/10.3390/en18195108
- Vasić, M. P., Matejic, M., & Blagojevic, M. (2018). Influence Analysis of Selected Turbine to Working Influence Analysis of Selected Turbine to Working Characteristics of Small Hydro Power Plants. *Machine Design*, 10(1), 11–16. https://doi.org/10.24867/MD.10.2018.1.11-16.
- Verde, A., Lastres, O., Hernández, G., Ibañez, G., Verea, L., & Sebastian, P. J. (2018). A new method for characterization of small capacity wind turbines with permanent magnet synchronous generator: An experimental study. *Heliyon*, 4(8). https://doi.org/10.1016/j.heliyon.2018.e00732
- Wendimu, A., Yoseph, T., & Ayalew, T. (2023). An overview of the role of irrigation in the attainment of sustainable development goals through hunger and poverty alleviation in Ethiopia. *International Journal of Innovative Research and Scientific Studies*, 6(4), 980–993. https://doi.org/10.53894/ijirss.v6i4.2215
- Wu, R. C., Tseng, Y. W., & Chen, C. Y. (2018). Estimating parameters of the induction machine by the polynomial regression. Applied Sciences, 8(7), 1073. https://doi.org/10.3390/app8071073



© 2025. The Author(s). This article is an open access article distributed under the terms and conditions of the Creative Commons Attribution-ShareAlike 4.0 (CC BY-SA) International License (http://creativecommons.org/licenses/by-sa/4.0/)